Atherosclerosis 289 (2019) 73–84

Contents lists available at ScienceDirect

Atherosclerosis

journal homepage: www.elsevier.com/locate/atherosclerosis

Forced expression of microRNA-146b reduces TRAF6-dependent inflammation and improves ischemia-induced neovascularization in hypercholesterolemic conditions

Michel Desjarlais[a], Sylvie Dussault[a], François Rivard[a], Sharon Harel[b], Veronica Sanchez[b], Sabah N.A. Hussain[b], Alain Rivard[a,*]

[a] Department of Medicine, Centre Hospitalier de l'Université de Montréal (CHUM) Research Center, Montréal, Québec, Canada
[b] Department of Medicine, McGill University Health Center, Montréal, Québec, Canada

HIGHLIGHTS

- Neovascularization is impaired in animal models and patients presenting hypercholesterolemia.
- MicroRNA-146b is reduced by hypercholesterolemia, which leads to TRAF6-dependent inflammation and impaired angiogenesis.
- Forced expression of miR-146b could reduce inflammation and improve neovascularization in atherosclerotic conditions.

ARTICLE INFO

Keywords:
Angiogenesis
Inflammation
Hypercholesterolemia
microRNA
Neovascularization

ABSTRACT

Background and aims: MicroRNA (miR)-146 is a key regulator of inflammation, endothelial activation and atherosclerosis. This study sought to define its potential role for the modulation of ischemia-induced neovascularization in atherosclerotic conditions.

Methods: Next generation sequencing and qRT-PCR analyses were used to compare microRNA expression in the ischemic muscles of hypercholesterolemic ApoE-deficient ($ApoE^{-/-}$) mice *vs.* wild type mice, and in HUVECs exposed or not to oxLDL. Neovascularization was investigated in a mouse model of hindlimb ischemia and the functional activities of HUVECs and pro-angiogenic cells (PACs) were assessed *in vitro*.

Results: We found that miR-146b (but not miR-146a) is significantly reduced in the ischemic muscles of $ApoE^{-/-}$ mice, and in HUVECs exposed to oxLDL. Inhibition of miR-146b reduces angiogenesis *in vitro*, whereas forced expression of miR-146b rescues oxLDL-mediated impairment of endothelial cell proliferation and tube formation. Mechanistically, miR146b directly targets tumor necrosis factor-alpha (TNFa) Receptor Associated Factor 6 (TRAF6) to inhibit inflammation. We found that hypercholesterolemia and oxLDL exposure are associated with higher levels of TRAF6, and increased expression of TNFa. However, forced expression of miR-146b in high cholesterol conditions reduces the expression of these inflammatory factors. *In vivo*, intramuscular injection of miR-146b mimic reduces ischemic damages and restores blood flow recuperation and capillary density in the ischemic muscles of $ApoE^{-/-}$ mice. Treatment with miR-146b also increases the number and functional activities of pro-angiogenic cells (PACs).

Conclusions: Hypercholesterolemia is associated with reduced expression of miR-146b, which increases TRAF6-dependent inflammation and is associated with poor neovascularization in response to ischemia. Forced expression of miR-146b using a miR mimic could constitute a novel therapeutic strategy to improve ischemia-induced neovascularization in atherosclerotic conditions.

1. Introduction

Atherosclerosis is a chronic inflammatory vascular disease characterized by the growth of lipid-rich plaques that cause narrowing of blood vessels and eventually lead to tissue ischemia. Immune cells dominate early atherosclerotic lesions, but inflammation is also involved in the progression of the disease and the triggering of acute ischemic events [1–3]. Until recently, the inflammatory hypothesis of

* Corresponding author. Centre de recherche du CHUM, Tour Viger, R08.464900 rue St-Denis, Montreal, Quebec, H2X 0A9, Canada.
E-mail address: alain.rivard@umontreal.ca (A. Rivard).

https://doi.org/10.1016/j.atherosclerosis.2019.08.010
Received 24 January 2019; Received in revised form 29 July 2019; Accepted 22 August 2019
Available online 23 August 2019

atherothrombosis remained unproved. However, the landmark CANTOS clinical trial recently showed that anti-inflammatory therapy targeting the interleukin-1β innate immunity pathway with canakinumab significantly reduces the rate of recurrent cardiovascular events, independently of lipid-level lowering [4]. These findings could open up a whole new avenue for the treatment of cardiovascular diseases. However, to improve the efficacy and specificity of anti-inflammatory therapies in vascular diseases, it will be important to define the precise factors and mechanisms that are involved in different clinical settings, including the response to ischemia.

Risk factors such as hypercholesterolemia are associated with inflammatory activation of endothelial cells (ECs) and endothelial dysfunction [5], the first manifestation of atherosclerotic diseases. Activated ECs use the nuclear factor κ light chain enhancer of activated B cells (NF-κB) pathway [6] to propagate inflammatory signals, including induction of adhesion molecules such as vascular cell adhesion molecule-1 (VCAM-1), intercellular adhesion molecule-1 (ICAM-1) and E-Selectin [5]. MicroRNAs are increasingly recognized as important regulators of inflammatory pathways and EC activation. microRNA-146a (miR-146a) has been well characterized in both ECs and leukocytes as a negative regulator of NF-κB activity through its ability to target upstream adaptor proteins, including TRAF6 (TNF receptor–-associated factor 6) and IRAK1 (interleukin receptor–associated kinase 1) [7,8]. miR-146a blunts endothelial activation [7] and protects against atherosclerosis [9,10]. miR-146b was also recently shown to modulate inflammatory responses in endothelial cells [11].

When atherosclerotic lesions are severe and diffuse, neovascularization constitutes a crucial physiological response in order to maintain the perfusion and the integrity of tissues [12]. Neovascularization necessitates the proliferation and the migration of mature endothelial cells that extend the pre-existing vascular network (i.e. angiogenesis) [13]. In addition to angiogenesis, postnatal neovascularization also depends on the action of bone marrow-derived pro-angiogenic cells (PACs) [14,15]. PACs can reach ischemic sites where they promote neovascularization mainly through paracrine secretion of cytokines and growth factors [16].

Risk factors and pathological conditions involved in the development of atherosclerosis are also often associated with impaired neovascularization following ischemia [12]. Hypercholesterolemia, one of the most important cardiovascular risk factor, has been associated with reduced angiogenesis and blood flow recuperation in several animal models [17–19]. Even in patients without apparent atherosclerotic diseases, hypercholesterolemia by itself was shown to reduce the number and the function of PACs [20]. Although inflammation has been linked mechanistically to hypercholesterolemia, oxidized LDL (oxLDL) and the atherosclerotic process [1–3], its potential influence on the modulation of ischemia-induced neovascularization in high-cholesterol conditions is unknown. Moreover, the role of specific microRNAs in these situations remains to be determined. In the present report, we identified miR-146b as an anti-inflammatory miRNA which expression is significantly reduced in hypercholesterolemic conditions. This is associated with activation of TRAF6-dependent inflammation, impaired angiogenic activities of mature endothelial cells and PACs, and poor neovascularization in response to ischemia. Our results also suggest that forced expression of miR-146b could represent a novel therapeutic strategy to reduce inflammation and improve neovascularization in atherosclerotic vascular diseases.

2. Materials and methods

2.1. Cell culture

Human umbilical vein endothelial cells (HUVECs) were purchased from Life Technologies (Carlsbad, CA) and cultured in medium 200 (Life technologies) supplemented with 8% fetal bovine serum (FBS, Wisent, St-Jean-Baptiste, QC, Canada), 100 IU/ml penicillin/0.1 mg/ml streptomycin (Wisent) and low serum growth supplement (LSGS; 2% FBS, 3 ng/ml bFGF, 10 mg/ml heparin, 1 mg/ml hydrocortisone, and 10 ng/ml EGF; Life Technologies). In some experiments, HUVECs were treated with oxLDL (50 μg/ml, Biomedical Technologies). HUVECs were passaged when they reached 90% confluence and passages 3–6 were used for all experiments. Human leukemia monocyte cell lines (THP-1) were cultured in RPMI 1640 (Wisent #350-000-CL) supplemented with 10% FBS, 100 IU/ml penicillin/0.1 mg/ml streptomycin. HUVECs and THP-1 cells were grown at 37 °C, 5% CO_2 and 95% air, and the medium was changed every 2 days.

2.2. RNA isolation and next generation sequencing analyses

RNA was extracted from ischemic hindlimb muscles (1 day after surgery) using the Ambion mirVana™ miRNA isolation kit (Life Technologies) according to the manufacturer's protocol. Quantification of total RNA was made with a nanodrop and 1 μg of total RNA was used for library preparation. Quality of total RNA was assessed with the BioAnalyzer Nano (Agilent) and all samples had a RIN above 8. Library preparation was done with the Truseq Small RNA library preparation kit (Illumina, Cat no. RS-200-0012). 11 PCR cycles were required to amplify libraries. Libraries were quantified with a nanodrop and the quality was assessed with the BioAnalyzer High Sensitivity (Agilent). All libraries were diluted to 10 nM, normalized and pooled to equimolar concentration based on Miseq v2 50 cycles using 7 pM of pooled library. Sequencing was performed with the Illumina Hiseq2000 using the Hiseq Reageant Kit v3 (200 cycles, paired-end) and 1.7 nM of the pooled library. Around 70 M paired-end reads was generated per sample. Quantification includes the raw read count, as well as normalized expression level as RPM values (reads per million reads mapped) to account for the variability in the library size. Next Generation Sequencing (NGS) data have been deposited and are available on NCBI Gene Expression Omnibus, GSE131002.

2.3. qRT-PCR evaluation of miRNA and mRNA expression

For the evaluation of miRNA expression, total RNA was reverse transcribed using the TaqMan® MicroRNA Reverse Transcription Kit (Life Technologies) as described by the manufacturer. Before use, RT samples were diluted 1:5. miR-146b gene expression level was determined using Taqman MicroRNA assays (Cat. # 4427975, Life Technologies). qPCR reactions were performed with cDNA samples using Perfecta qPCR Fastmix II (Quanta) and specific miR-146b primers. The Viia7 qPCR instrument (Life Technologies) was used to detect the amplification level. Relative expression ($RQ = 2^{-rrCT}$) was calculated using the Expression Suite software (Life Technologies), and normalization was done using both U6 snRNA and SnoRNA 202. For mRNA gene expression, total RNA was extracted from HUVECs using RNeasy mini kit (Qiagen) according to the manufacturer's protocol. The RNA was reverse transcribed using iScript-II RT kit (Qiagen) according to manufacturer's guidelines to generate cDNA. Quantitative real-time PCR was performed using cDNA sample, specific primers for the selected mRNAs (Alpha DNA, Montreal, Canada) and Universal SYBR Green Supermix (BioRad). Relative expression ($RQ = 2^{-rrCT}$) was calculated using the instrument detection system ABI Prism 7500 (Applied Biosystems, Foster City, CA, USA) and normalized to b-Actin and 18s.

2.4. miRNA and siRNA transfection in HUVECs

Transfections were carried out at a concentration of 50 nM using Lipofectamine RNAiMAX Reagent (Life Technologies) according to the manufacturer's protocol and as previously described [21]. HUVECs were transfected 24 h after being plated in 6-well plates with the following miRs purchased from Dharmacon (GE Healthcare Dharmacon, Lafayette, CO): miRIDIAN miR mimic negative control #1, miRIDIAN miR mimic hsa-miR146b-5p, miRIDIAN anti-miR negative control #1,

miRIDIAN anti-miR hsa-miR146b-5p hairpin inhibitor. siRNAs were purchased from Thermo fisher Scientific (Thermo fisher Scientific, Grand island, NY): silencer siRNA control, siRNA anti-TRAF6. After 24 h, the transfection medium was replaced with antibiotic-free complete M200 medium and cells were exposed or not to 50 μg/ml of oxLDL for 24 h. For luciferase assay experiments, miRNA transfection was performed 24 h after vector transfection. Transfection efficiency was measured using mimic transfection control Dy547 (Dharmacon) and found to be 80–90%.

2.5. Luciferase constructs and vector transfection

3′ UTR Luciferase construct pMIR-REPORT^{TM} plasmid containing 500 bp of wild-type 3′ UTR of TRAF6 (TRAF6-wt UTR) was cloned downstream of a CMV-driven Firefly Luciferase cassette [11]. A mutated version of this construct (TRAF6- mut-UTR) carrying a 4-bp substitution in the miR-146b target sites was constructed by site-directed mutagenesis [11]. HUVECs were transfected (50 nM) for 24 h according to the manufacturer's protocol using Lipofectamine RNAiMAX Reagent (Life Technologies) and a luciferase construct (TRAF6-wt UTR or TRAF6-mut UTR), together with a Renilla luciferase control vector (pRL-TK). HUVECs were then allowed to recover for 24 h in complete medium before treatment with oxLDL (50 μg/ml) or transfection with miR-146b mimic. Firefly and Renilla luciferase activities were quantified using a Dual-Luciferase Reporter Assay System and Firefly luciferase activity was normalized for renilla activity to control for transfection efficiency differences.

2.6. Detection of intracellular reactive oxygen species (O_2^-)

Generation of superoxide anions (O_2-) in HUVECs were assessed with the fluoroprobes dihydroethidium (DHE, Molecular probes). Fluorescence intensities were quantified using image J, with the same threshold for each experiment.

2.7. THP-1 monocyte adhesion assay

Monocyte adhesion to ECs was assessed by co-incubation of THP-1 and HUVECs for 1 h. Briefly, 50 000 THP-1 cells pre-stained with Calcein AM (Life Technologies) where co-incubated with confluent HUVECs in 24-well plates. Cells were washed three times with PBS and adherent THP-1 cells were counted in 10 fields per well using fluorescence microscopy. Before the incubation with THP-1 cells, HUVECs were transfected or not with miR-146b mimic, anti-miR-146b or appropriate controls for 24 h and exposed or not to 50 μg/ml oxLDL for 24 h.

2.8. HUVEC capillary-like tube formation on matrigel

The angiogenic activity of HUVECs was determined using a Matrigel tube formation assay. Briefly, after transfection, HUVECs were plated at a density of 20 000 cells/well in 96-well plates precoated with 50 μl of growth factor reduced Matrigel Matrix (Becton Dickinson Labware, Bedford, MA) and cultured at 37 °C for 24 h with 10% FBS. HUVECs were transfected or not with miR-146b mimic, anti-miR-146b or appropriate controls for 24 h, and exposed or not to 50 μg/ml oxLDL for 24 h. Capillary-like tubes were observed under a light microscope. Images were obtained at a 50x magnification, and all tubes were counted.

2.9. Scratch assay

Measurement of cell migration was performed using an adapted scratch assay in confluent HUVECs. The cells were transfected and grown to near confluence in 24-well plates and exposed or not to 50 μg/ml oxLDL. Mechanical disruption of the monolayer was realized by scraping with a pipette tip. Migration was assessed using an inverted microscope at a magnification of 200x by an investigator blinded to the experimental conditions. Three fields per well were evaluated and all experiments were performed in duplicate.

2.10. Murine ischemic hindlimb model

The protocol was approved by the Comité Institutionnel de Protection des Animaux (CIPA) of the Centre Hospitalier de l'Université de Montréal (CHUM). 6 to 8 week-old hypercholesterolemic *ApoE*$^{-/-}$ mice were purchased from Jackson Laboratory (Bar Harbor, ME) and put on a western-type diet (1.25% cholesterol, 15% cocoa butter, 0.5% sodium cholate, Teklad 90221) for 5 weeks before the surgery. Unilateral hindlimb ischemia was surgically induced after anesthesia with 2% isoflurane as previously described [22]. Mice were injected intramuscularly [21] with 5 mg/kg of in vivo ready mirVana® miRNA mimic mmu-miR146–5p, or mirVana® miRNA mimic negative control #1 (Life technologies). This dose was chosen based on preliminary experiments showing optimal transfection efficiency in muscles [21]. miRNAs were administered in a solution of Max suppressor RNA-LANCEr II (Bioo Scientific, Austin, TX) according to the manufacturer's recommendations. Ischemic damages were evaluated using a scale from 1 (no damage) to 4 (lost fingers). The mice were killed at predetermined arbitrary time points after surgery with an overdose of sodium pentobarbital.

2.11. Monitoring of blood flow

Hindlimb blood flow (6–8 mice/group) was monitored with a Laser Doppler perfusion imager (LDPI) system (Moor Instrument Ltd., Axminster, UK) after anesthesia with a ketamine-dexmedetomidine solution (50 mg/kg and 0.5 mg/kg, IP) [22]. Laser Doppler measurements were performed by a single observer blinded to the treatment group at day 7 after surgery. After LDPI measurements, dexmetedomidine was antagonized with a solution of Atopamezole (1 mg/kg, SC). To account for variables such as ambient light and temperature, the results are expressed as the ratio of perfusion in the left (ischemic) *vs.* right (non-ischemic) hindlimb.

2.12. Capillary histochemistry

Whole ischemic hindlimbs were harvested 7 days after surgery and immediately fixed in Tissufix (Chaptec, Montreal, QC, Canada) overnight. After bones were carefully removed, 3 mm thick tissue transverse sections of the hindlimbs were cut at the level of the gastrocnemius muscle and paraffin-embedded so that the whole leg could be analysed on each section. Identification of endothelial cells was performed by immunohistochemistery for CD31 with a rat monoclonal antibody directed against mouse CD31 (BD Pharmigen, San Diego, CA, USA). Negative control was perform in same condition without the primary antibody (CD31). Capillaries were counted by a single observer blinded to the treatment regimen at a 200x magnification. Results are expressed as the number of capillaries per field.

2.13. PAC isolation and characterization

7 days after hindlimb ischemia, mouse bone marrow mononuclear cells were isolated from the femora and tibiae by flushing the bone marrow cavities using culture medium, and kept on fibronectin-coated (Sigma, St. Louis, MO) plates. After 4 days in culture, non-adherent cells were removed by thorough washing with PBS. Adherent cells were stained with DAPI (0.5 mg/ml; Life Technologies),1,10-dictadecyl-3,3,30,30 acetylated low-density lipoprotein (DiI-acLDL, 2.5 mg/ml for 1 h, Life Technologies) and FITC-labelled lectin BS-1 (Bandeiraea simplicifolia, 10 mg/ml for 1 h, Sigma, St-Louis, MO). Bone marrow PACs were characterized as adherent cells that were positive for both DiI-

acLDL uptake and lectin binding as previously described [22].

2.14. PAC adhesion to an endothelial monolayer

A monolayer of HUVECs (passage 4–6) was prepared in 24 well plates. HUVECs were pretreated for 16 h with tumour necrosis factor-a (1 ng/ml; BD Biosciences), fixed and stained with DAPI (0.5 mg/ml; Life Technologies). PACs were labelled with DiI-AcLDL and 15 000 cells were added to each well (2 wells/mouse) and incubated for 3 h at 37 °C. Non-attached cells were gently removed with PBS and adherent PACs were fixed with 2% paraformaldehyde and counted in three random fields per well [22].

2.15. Incorporation of PACs into HUVECs tubules

PACs (3000) labelled 1 h with DiI-acLDL were co-plated with HUVECs (20 000) in 96-well plates that had been precoated with 50 µl of growth factor reduced Matrigel Matrix (Biosciences, San Diego, CA, USA) and cultured at 37 °C for 24 h with 10% FBS. Tubular-like structures were photographed and the number of incorporated EPCs was determined in 6 random fields. A tube was defined as a straight cellular segment connecting two cell masses (nodes). No difference in the total number of tubes or in tube length was observed between the different groups (data not shown). The data are presented as number of incorporated EPCs/tube [22].

2.16. PAC proliferation assay

PAC proliferative capacity was determined using MTS (Celltiter 96 aqueous non-radioactive cell-proliferation) assay obtained from Promega (Madison, WI). Briefly, 30 000 PACs were plated in 96 well plates and incubated for 24 h with 10% FBS. MTS was added to each well to achieve a final concentrations of 0.04 mg/ml. Proliferation was quantified after 4 h by densitometric analysis of MTS tetrazolium compound. Optical density was recorded with a microplate reader at 490 nm. Readings were corrected for background optical density by subtracting the readings from EBM/MTS incubated at the same time in the absence of PACs.

2.17. Western blot analysis

Protein levels were analysed by Western blots in ischemic muscle homogenates and in HUVEC extracts. For total protein extraction, isolated muscles from whole hindlimbs were rinsed in PBS to remove excess blood, snap-frozen in liquid nitrogen, and stored at −80 °C until use. Whole-cell protein extracts were obtained after homogenization of ischemic muscles of the different groups of mice in ice cold RIPA buffer (pH = 8) containing 50 mM Tris-HCL, 150 mM NaCl, 5 mM EDTA, 1% Triton 100x, 0.5% sodium deoxycholate, 0.1% SDS with a cocktail of proteases and phosphatases inhibitors (MiniComplete, PhosphoStop and PMSF, Roche, Bâle, Switzerland). HUVECs were lysed with 50 µl of RIPA lysis buffer per well in 6-well plates, harvested and sonicated. 50 µg of protein per muscle homogenate sample and 20 µg of protein per cell lysate sample were separated on an SDS-polyacrylamide gel and electroblotted on nitrocellulose membranes. Non-specific binding sites were blocked with 5% skim milk powder in TBS-T (50 mM Tris-HCL, 140 mM NaCL, 0.05% Tween 20) for 1 h. The membranes were probed overnight at 4 °C with the following antibodies: TRAF6 (1:1000, Cell signaling Technology, Danvers, MA), TNFa (1:1000, phosphoTYR146-SRC, Cell signaling Technology, Danvers, MA), or β-actin (1:2000, Santa Cruz Biotechnology). Membranes were then washed three times for 10 min with TBS-T and incubated with secondary antibodies conjugated with HRP (1:2000) for 1 h and washed with TBS-T. Specific proteins were detected by chemiluminescent reaction (GE Healthcare, Piscataway, NJ) followed by exposure to Hyperfilm ECL (GE Healthcare). Protein expression was quantified using ImageJ and the results are expressed as density values normalized to the loading control (β-actin).

2.18. Statistical analysis

All results are mean ± SEM. Statistical significance was evaluated by unpaired *T* test or ANOVA followed by a Newman Keuls post hoc test. A value of $p < 0.05$ was interpreted to denote statistical significance.

3. Results

3.1. Effect of hypercholesterolemic conditions on miR-146 expression

Next generation sequencing (NGS) was used to evaluate the expression of miRNAs in ischemic hindlimb muscles of hypercholesterolemic ApoE-deficient ($ApoE^{-/-}$) mice compared to normocholesterolemic control mice. miRNAs with at least 1000 reads per million reads mapped-(RPM) and modulated by 20% or more were included in the analysis. Hypercholesterolemia was mainly associated with downregulation of miR expression in ischemic muscles (Supplemental Fig. 1). Only 10 miRs were upregulated compared to 71 miRs that were downregulated. Moreover, among the 10 upregulated miRs, 8 are not expressed in humans and the other two were modulated by only 20–25%. Therefore we chose to focus on downregulated miRs. As seen on Fig. 1A and Supplemental Fig. 1, miR-146b was highly expressed in ischemic muscles and one of the most downregulated miRs in hypercholesterolemic conditions. By contrast, miR-146a was not significantly modulated in hypercholesterolemic conditions (Fig. 1A). miR-146b is expressed in mammals, including mice and humans. Using qRT-PCR, we confirmed that the expression of miR-146b is significantly impaired in the ischemic muscles of hypercholesterolemic $ApoE^{-/-}$ mice (Fig. 1B). The expression of miR-146b is also significantly reduced in human umbilical vein endothelial cells (HUVECs) exposed to oxLDL (Fig. 1C and Supplemental Fig. 3A). Interestingly, miR-146 was previously found to modulate the inflammatory responses in endothelial cells [7,11]. In the following experiments, we focused on characterizing the role of miR-146b in the modulation of inflammation, angiogenesis and neovascularization in atherosclerotic/hypercholesterolemic conditions.

3.2. miR-146b rescues angiogenesis in endothelial cells exposed to oxLDL

To study the role of miR-146b *in vitro*, we performed gain- and loss-of-function experiments by transfecting HUVECs with a miR-146b mimic or an anti-miR-146b. Transfection efficiency was established to be more than 80%, as assessed using a labelled miRNA mimic control (data not shown). As seen on Fig. 2A and E, exposure to oxLDL reduces tube formation in HUVECs. However, treatment with miR-146b significantly improves tube formation in HUVECs exposed to oxLDL. In addition, miR-146b rescues oxLDL-induced impairment of cell migration in HUVECs (Fig. 2B and F). On the other hand, similarly to oxLDL exposure, inhibition of miR-146b in HUVECs leads to impaired tube formation (Fig. 2A and E) and cellular migration (Fig. 2B and F). miR146 is known to repress endothelial activation by inhibiting pro-inflammatory pathways [7]. Here we found that in HUVECs that are exposed to oxLDL, miR-146b treatment significantly reduces monocyte adhesion (Fig. 2C and G) and oxidative stress levels (Fig. 2D and H). By opposition, inhibition of miR-146b promotes monocyte adhesion and oxidative stress in HUVECs (Fig. 2C–H).

3.3. miR-146b directly targets TRAF6 and inhibits oxLDL-induced TRAF6-TNFa inflammatory pathway

miR-146a and miR-146b have previously been shown to target and induce post-transcriptional repression of TNF receptor–associated

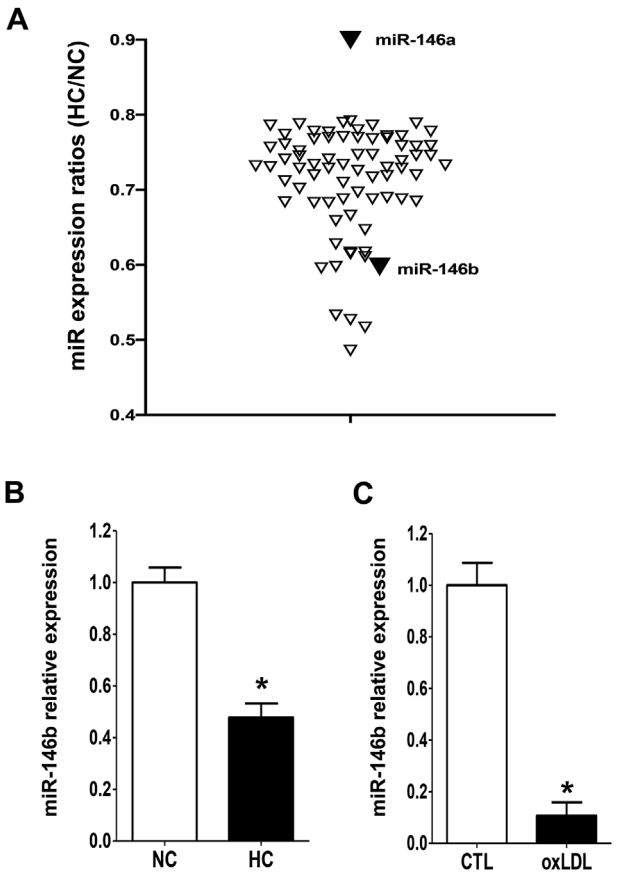

Fig. 1. Effect of hypercholesterolemic conditions on miR-146b expression. (A) Relative expression of downregulated miRNAs (pool of 3 mice/group) in the ischemic muscles of hypercholesterolemic ApoE knockout mice (HC) *vs.* normocholesterolemic control mice (NC) as assessed by next generation sequencing (NGS). (B, C) Relative expression of miR-146b in ischemic muscles of NC and HC mice (n = 3) (B) and in HUVECs exposed or not to 50 μg/ml oxLDL (C) (n = 3) as quantified by real-time qPCR. CTL = controls. Data are mean ± SEM. *$p < 0.05$ *vs.* CTL or NC.

factor 6 (TRAF6) [8]. We found that TRAF6 and TNFa are significantly increased in the ischemic muscles of hypercholesterolemic *ApoE*$^{-/-}$ mice compared to normocholesterolemic control mice (Fig. 3A). *In vitro*, there is a rapid induction of TRAF6 and TNFa in HUVECs that are exposed to oxLDL (Fig. 3B). Interestingly, inhibition of miR-146b induces a similar increase in the expression of TRAF6 and TNFa in control HUVECs not treated with oxLDL (Fig. 3C). On the other hand, treatment with a miR-146b mimic can prevent the activation of TRAF6-TNFa inflammatory pathway in HUVECs exposed to oxLDL (Fig. 3D). Using specific luciferase assays in HUVECS, we found that miR-146b directly targets wild-type TRAF6, but not a TRAF6 construct where miR-146b target site has been mutated (Fig. 4A and B). Our results also indicate that the increase of TRAF6 expression following oxLDL exposure is at least in part miR-146b dependent, since TRAF6 induction by oxLDL (Fig. 4C, left panel) is not seen when miR-146b target site is mutated (Fig. 4C, right panel). Finally, we found that inhibiting TRAF6 using a siRNA reduces inflammation and improves endothelial cell migration and tube formation in HUVECs that are treated with anti-miR-146b (Supplemental Fig. 2). This confirms the role of TRAF6 in the modulation of EC function by miR-146b.

3.4. miR-146b treatment improves ischemia-induced neovascularization in hypercholesterolemic conditions

We and others have previously shown that ischemia-induced neovascularization and blood flow recuperation are impaired in hypercholesterolemic *ApoE*$^{-/-}$ mice [18,21]. To investigate the potential beneficial effect of miR-146b in vivo, hindlimb ischemia was surgically-induced in hypercholesterolemic *ApoE*$^{-/-}$ mice and blood flow perfusion was evaluated by Laser Doppler perfusion imaging (LDPI) studies in mice treated intramuscularly with miR-146b mimic or a miR control (Fig. 5 and Supplemental Fig. 3B). As shown on Fig. 5A and B, *ApoE*$^{-/-}$ mice treated with miR-146b mimic showed a significant improvement of blood flow recuperation at day 7 after surgery compared to those treated with a scrambled miR mimic control (Doppler flow ratio (DFR) 0.42 ± 0.02 *vs.* 0.33 ± 0.03; $p < 0.05$). Clinically, this was correlated with a reduction of ischemic damage in mice treated with miR-146b mimic (Fig. 5C). A similar effect was also observed at the microvascular level where intramuscular treatment with miR-146b mimic significantly increased vascular densities in the ischemic muscles of *ApoE*$^{-/-}$ mice (Fig. 5D and E). Moreover, we found that the expression of TRAF6 and TNFa were significantly reduced in the ischemic muscles of *ApoE*$^{-/-}$ mice treated with miR-146b mimic (Fig. 5F).

3.5. Effect of miR-146b treatment on the number and the functional activities of PACs in hypercholesterolemic conditions

PACs have been shown to reach ischemic sites where they can contribute to the formation of new blood vessels [16]. However the number and the functional activities of PACs are impaired in patients with atherosclerotic conditions, including hypercholesterolemia [20]. Here we found that the number of bone marrow-derived PACs is significantly increased in hypercholesterolemic *ApoE*$^{-/-}$ mice treated with miR-146b (Fig. 6A and D). Moreover the functional activities of PACs including proliferation (Fig. 6E), attachment to endothelial cells (Fig. 6B and F) and integration into endothelial cell tubules (Fig. 6C and G) were all improved in *ApoE*$^{-/-}$ mice treated with miR-146b mimic.

4. Discussion

To our knowledge, this is the first study demonstrating that hypercholesterolemia leads to reduced expression of an anti-inflammatory microRNA (i.e. miR-146b) in the context of ischemia. It is also the first documentation of the beneficial effect of microRNA therapy on ischemia-induced neovascularization through targeting of inflammatory signals in atherosclerotic conditions. Inflammation has been associated with classical risk factors such as hypercholesterolemia, and it is also involved in the development of atherosclerotic vascular diseases [1–3]. Recently it was shown that a specific anti-inflammatory therapy (i.e. antibody targeted at interleukin-1 beta) can reduce recurrent cardiovascular events in patients with a previous myocardial infarction [4]. However, whether anti-inflammatory treatments can also modulate the physiological response to ischemia (e.g. neovascularization) is currently unknown. Patients with atherosclerotic vascular diseases present several conditions that have been shown to impair ischemia-induced neovascularization [12]. Classical cardiovascular risk factors, including hypercholesterolemia, are associated with oxidative stress and inflammation [1–3]. These conditions can negatively modulate neovascularization, which could help explaining the lack of efficacy of pro-angiogenic therapies in clinical trials, compared to the positive results obtained in young and healthy animals [23]. Although miRs have previously been shown to modulate angiogenesis and neovascularization after ischemia [21], the present study is the first one documenting the role of a miR targeting inflammation (and more specifically TRAF6-dependent inflammation) on blood flow recovery and ischemia-induced neovascularization in an atherosclerotic context (hypercholesterolemia). Our study shows that reduced expression of the anti-inflammatory miR-146b contributes to impair neovascularization in hypercholesterolemic conditions. It also suggests that targeting inflammation through forced expression of specific miRNAs could constitute a novel therapeutic strategy to improve ischemia-induced

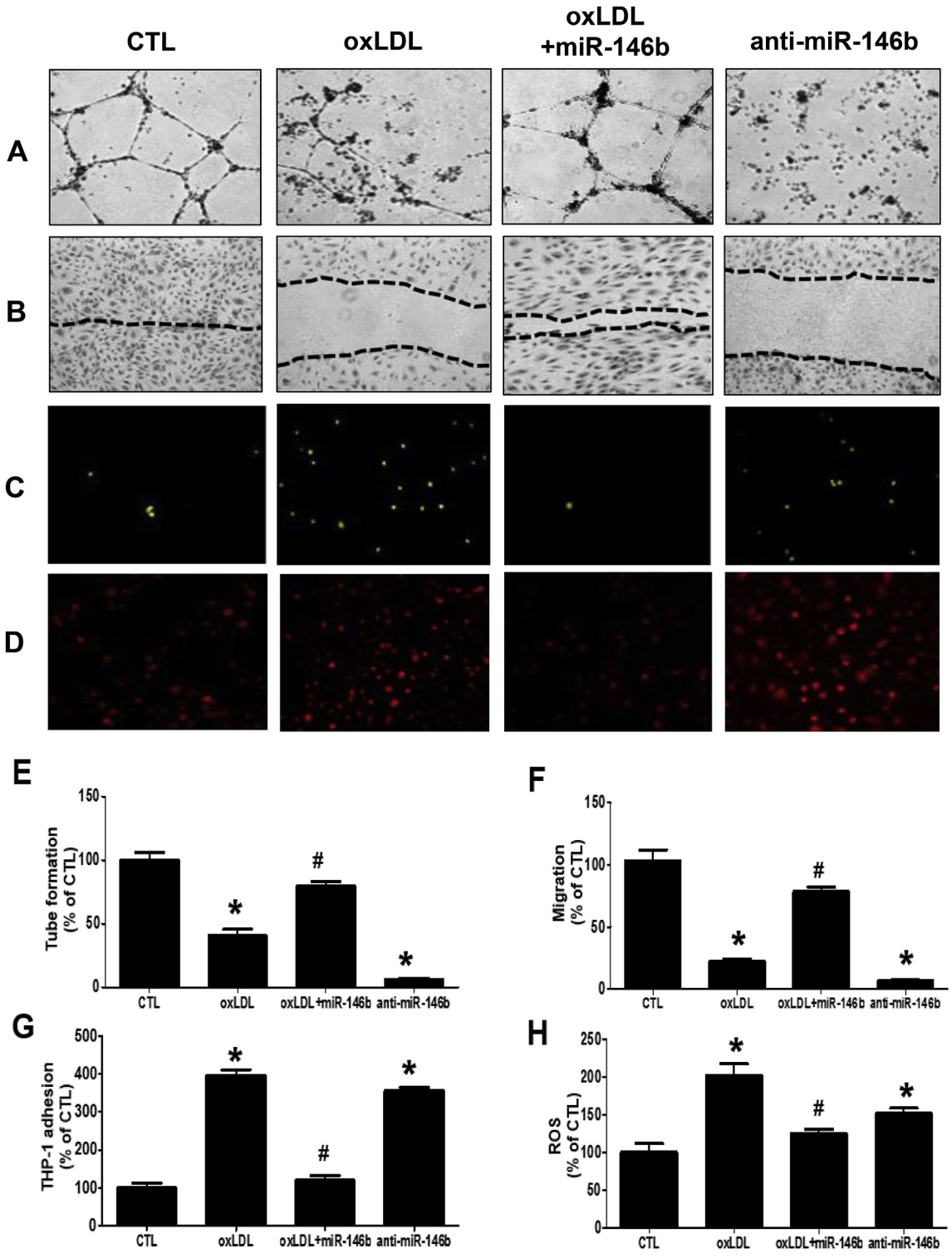

Fig. 2. Effect of oxLDL exposure and miR-146b modulation on endothelial cell function.
Evaluation of angiogenesis and cell migration *in vitro* using matrigel (A, E) and scratch (B, F) assays in HUVECs exposed or not to oxLDL (50 μg/ml) and treated or not with a miR-146b mimic or anti-miR-146b. Monocyte adhesion to endothelial cells was assessed after co-culture of THP-1 and HUVECs for 1 h (C, G). Superoxide anion generation in HUVECs was assessed using DHE staining (D, H). The control (CTL) and oxLDL groups were transfected with a scrambled miR control. Data are mean ± SEM (n = 4). *$p < 0.05$ *vs.* CTL; #$p < 0.05$ *vs.* oxLDL.

neovascularization in atherosclerotic conditions.

The miR-146 family of microRNAs consists of two member genes, miR-146a and miR-146b. These two microRNAs are located on different chromosomes and exhibit differential regulation in many cases [24]. Consistent with this, in the current study we found that miR-146b is significantly reduced in the ischemic muscles of $ApoE^{-/-}$ mice, whereas miR-146a is not modulated by hypercholesterolemia. This finding confirms that miR-146 family members have specific regulation and function that can vary depending on the conditions. Nonetheless, miR-146a and miR-146b are nearly identical in sequence, sharing a

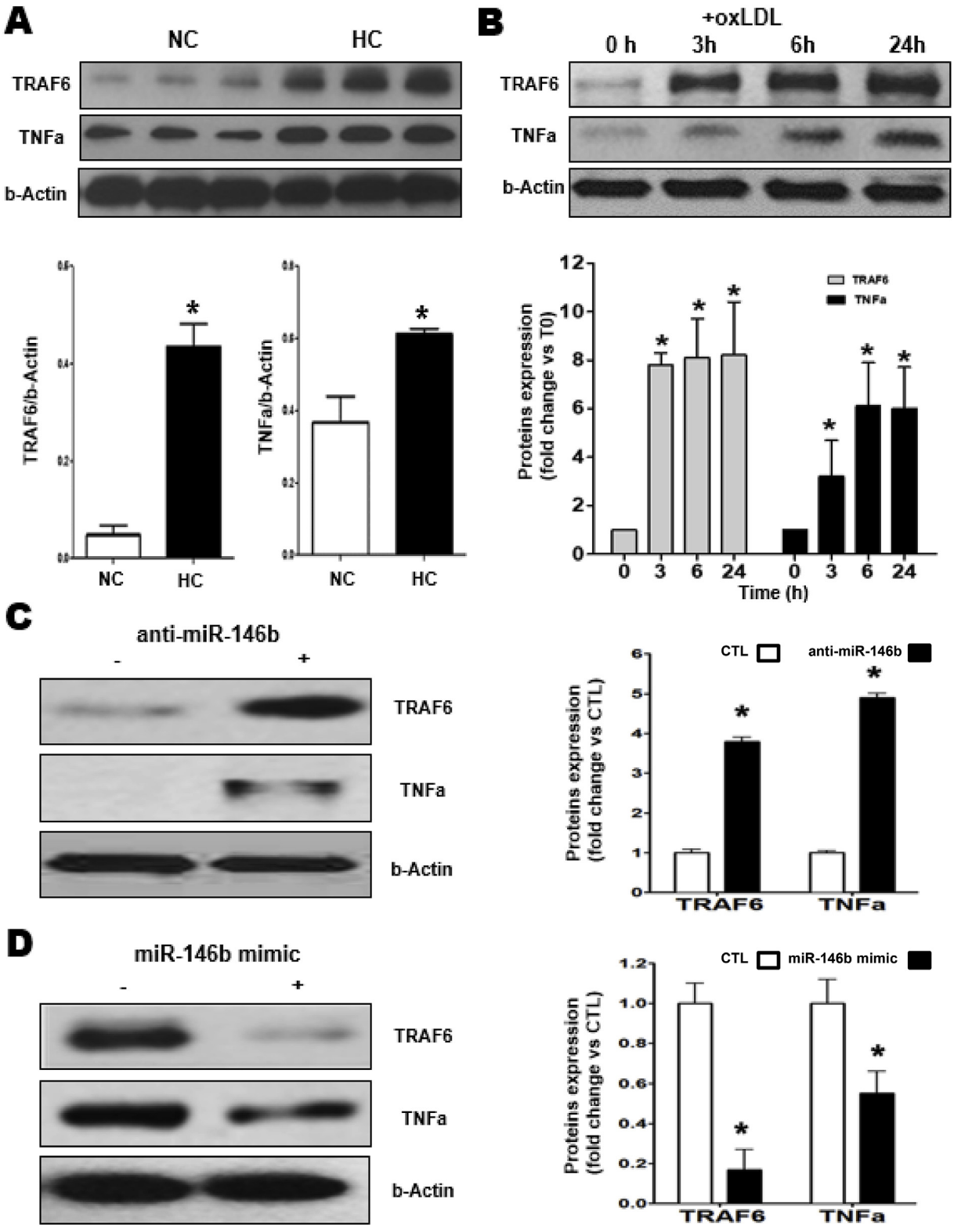

Fig. 3. miR-146b inhibits oxLDL-induced TRAF6-TNFa inflammatory pathway.
(A and B) Representative Western blots and quantitative analyses of TRAF6 inflammatory pathway in ischemic muscles of normocholesterolemic mice (NC) *vs.* hypercholesterolemic mice (HC) (A, n = 5), and in HUVECs treated or not with oxLDL (B, n = 4). (C) HUVECs were transfected with anti-miR-146b or a scrambled miR control (CTL). (D) HUVECs exposed to oxLDL were transfected with miR-146b mimic or a scrambled miR control (CTL). Data are mean ± SEM. $^{*}p < 0.05$ *vs.* CTL.

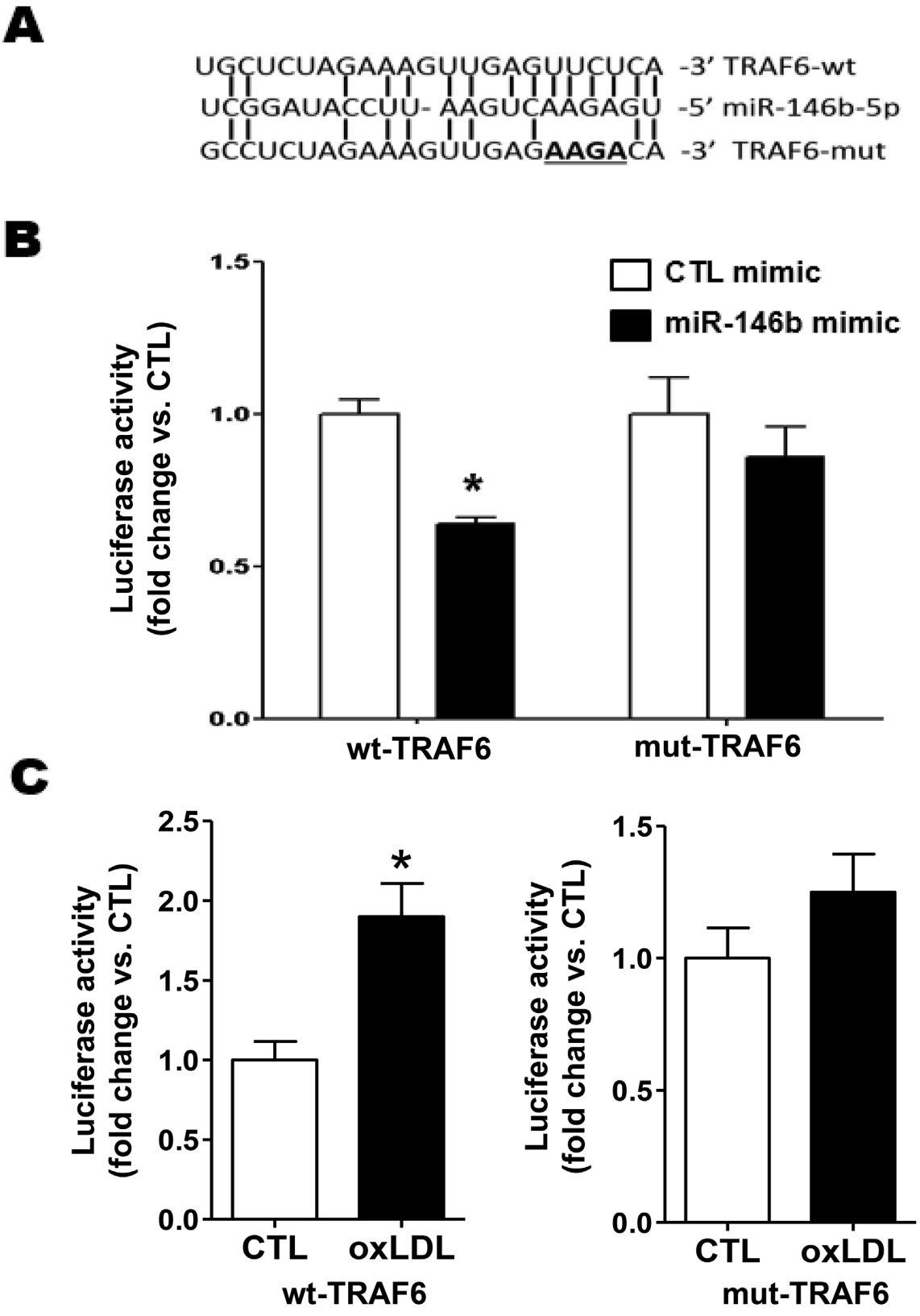

Fig. 4. miR-146b directly targets TRAF6 in endothelial cells.
(A) Schematic representation of TRAF6 target site for miR-146b (TRAF6-wt) and mutated target site construct of TRAF6 (TRAF6-mut). (B and C) Relative luciferase activity in HUVECs transfected with wt-TRAF6 or mut-TRAF6 constructs and treated or not with miR-146b mimic (B) or oxLDL (C). n = 4/group. Data are mean ± SEM. *$p < 0.05$ *vs.* CTL.

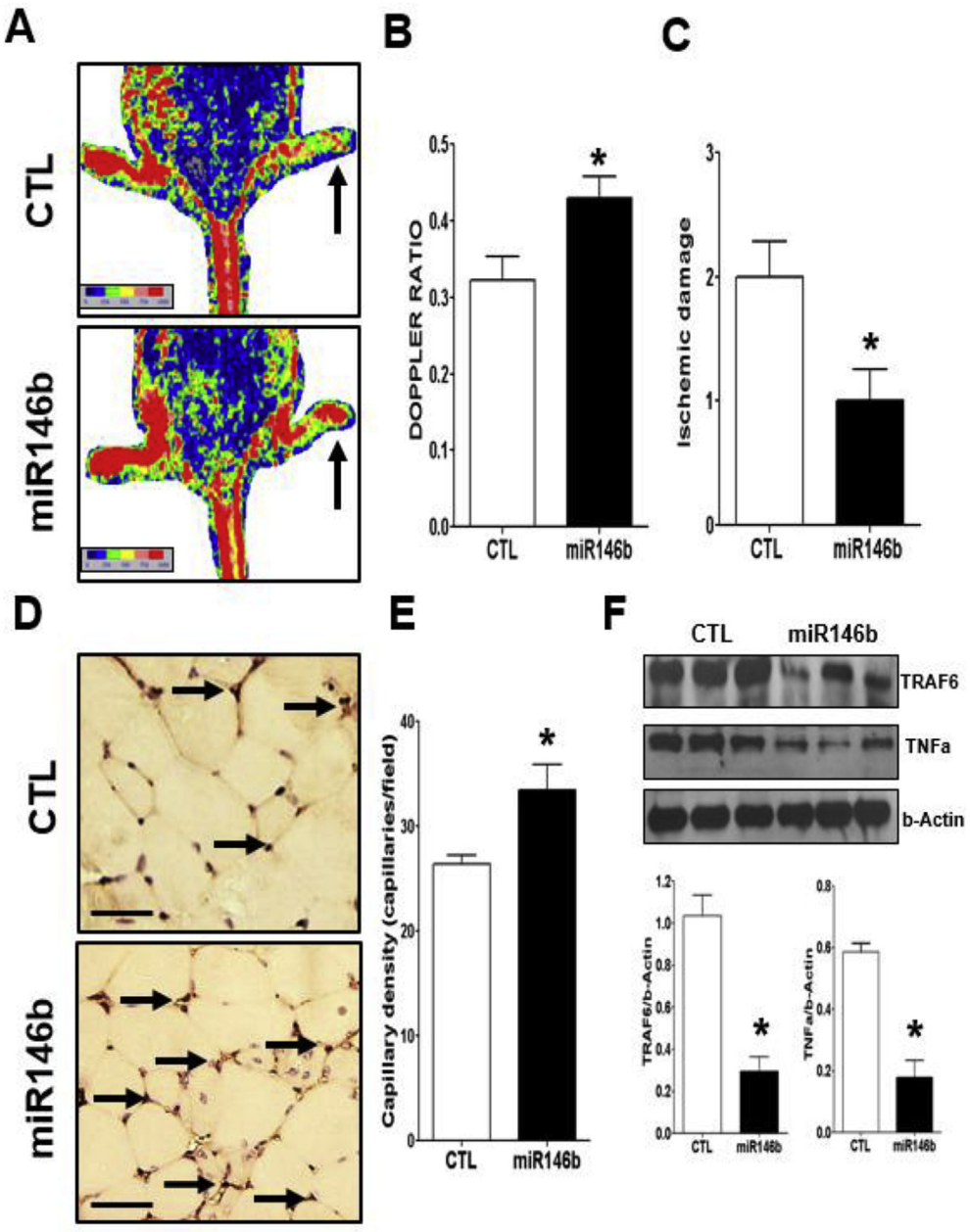

Fig. 5. Effect of miR-146b treatment on ischemia-induced neovascularization in hypercholesterolemic ApoE knockout mice. Quantification of blood flow recovery (Laser Doppler, A and B), ischemic damage (C) and capillary density (CD31 immunostaining, D and E) assessed 7 days after hindlimb ischemia in hypercholesterolemic mice treated with miR-146b mimic or a scrambled miR mimic control (CTL). Arrows indicate left ischemic hindlimb (A) and capillaries (D). (F) Representative Western blots and quantitative analyses of TRAF6 and TNFa expression in the ischemic muscles of the two groups of mice. Data are mean ± SEM (n = 6–8/group). *$p < 0.05$ *vs.* CTL. Scale bar = 50 μm.

seed region, and are thus predicted to target the same set of genes [8,24]. In the vascular system, miR-146a has been shown to blunt endothelial activation through repression of the pro-inflammatory NF-kB pathway [7]. Atheroprotective shear stress in ECs leads to increased miR-146a levels, and overexpressing miR-146a inhibits neointima formation after rat or mouse carotid artery injury [9]. Injection of miR-146a mimic into atheroprone mice was also shown to reduce atherosclerosis [10]. Although less extensively studied compared to miR-146a, miR-146b was recently shown to inhibit inflammatory responses in ECs through selective targeting of IRAK1 and TRAF6 [11]. Our study extends these previous findings and demonstrates that miR-146b is also crucial for the physiological response to tissue ischemia in hypercholesterolemic conditions. We found that the expression of miR-146b is reduced both in endothelial cells exposed to oxLDL and in the ischemic muscles of hypercholesterolemic *ApoE*$^{-/-}$ mice. Supplementation of miR-146b with a miR mimic could restore the angiogenic properties of endothelial cells exposed to oxLDL. More importantly, using a well characterized model of hindlimb ischemia, we show that miR-146b supplementation could have important therapeutic effects in ischemic tissues. *ApoE*$^{-/-}$ mice treated with miR-146b demonstrated significant improvement of blood flow recovery and reduced ischemic damage compared to controls. At the microvascular level, this was associated with increased capillary density in ischemic muscles of animals treated with miR-146b. Previous studies have suggested that miR-146a can promote the angiogenic activities of HUVECs *in vitro* [25–27]. However, our study constitutes the first documentation of the angiogenic properties of a miR-146 family member in vivo. Moreover, it is the first report focusing specifically on miR-146b angiogenic properties. We used a mouse model of ischemia-induced neovascularization in hypercholesterolemic conditions. Whether miR146b is also involved in the modulation of angiogenesis in other in vivo models such as tumor-related angiogenesis is currently unknown. In addition, although the current study focuses on endothelial cells, miR-146b can be expressed in different cell types and part of the effect of miR-146b on neovascularization could therefore be indirect through its action on other cell types such as myocytes and inflammatory cells.

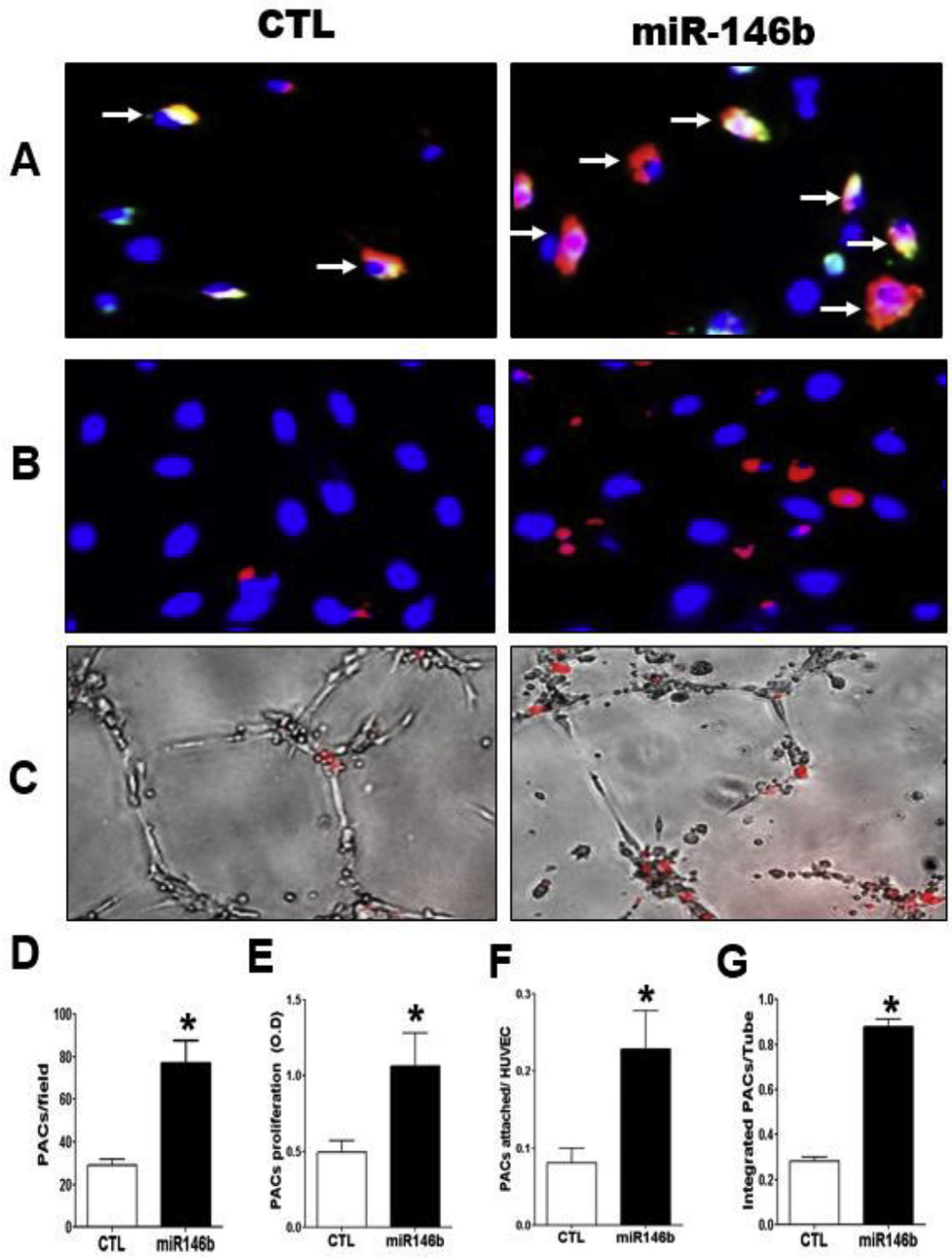

Fig. 6. Effect of miR-146b treatment on PAC number and function.
Representative pictures and quantification of PAC number (A, D), PAC (red) adhesion to HUVECs (B and F), PAC (red) integration into HUVEC tubules (matrigel assay, C and G) and PAC proliferation (MTS assay, E) in hypercholesterolemic ApoE knockout mice treated with a miR-146b mimic or a scrambled miR mimic control (CTL). Triple-stained PACs (DAPI, BS-1 lectin-FITC, and DiI-acLDL) are shown in (A). Data are mean ± SEM (n = 5/group). $^{*}p < 0.05$ *vs.* CTL.(For interpretation of the references to colour in this figure legend, the reader is referred to the Web version of this article.)

The mechanism by which miR-146b modulates angiogenesis and neovascularization after ischemia appears to involve TRAF6-TNFa inflammatory pathway. Both miR-146a and miR-146b are known to directly target TNF receptor–associated factor 6 (TRAF6) [8]. TRAF6 is an E3 ubiquitin ligase that acts as a signal transducer and induces NF-kappaB-dependent proinflammatory gene expression, including TNFa [28]. Although anti-angiogenic effects of TRAF6 have been described *in vitro* [29], its specific role for the modulation of ischemia-induced neovascularization is unknown. Here we found that reduced miR-146b levels correlate with increased expression of TRAF6 in the ischemic muscles of hypercholesterolemic mice and in HUVECs exposed to oxLDL. Using specific luciferase assays, we confirmed that TRAF6 is a direct target of miR-146b in endothelial cells. Our results also indicate that the modulation of TRAF6 expression following oxLDL exposure depends on miR-146b, as it necessitates a bona fide miR-146b target site within TRAF6. We found that increased levels of TRAF6 were also associated with induction of TNFa in endothelial cells exposed to oxLDL, which is consistent with previous results obtained in T cells [28]. Moreover, inhibiting TRAF6 reduced inflammation and improved angiogenesis in endothelial cells treated with anti-miR-146b, which confirms the role of TRAF6 in the modulation of EC function by miR-146b. Importantly, miR-146b treatment could reduce the expression of the inflammatory factors TRAF6 and TNFa *in vitro* and in vivo, and this was associated with improved angiogenesis and ischemia-induced neovascularization. The effect of inflammation on postnatal neovascularization is complex and context-dependent. Whereas inflammation can contribute to initiate angiogenesis, excessive inflammation is associated with the inhibition of reparative vessel growth in the setting of ischemia [30]. In particular, pro-inflammatory cytokines such IL-12 and IL-18 display anti-angiogenic properties [31]. The endogenous inhibitor of angiogenesis thrombospondin-1 (TSP-1) is also released during inflammatory processes. TSP-1 has been shown to limit the extent of neovascularization through inhibition of MMP-9 and impaired release of SDF-1 in a model of hindlimb ischemia [32]. TRAF6 has been shown

to inhibit angiogenesis *in vitro*, potentially through reduction of VEGF promoter activity and VEGF expression in endothelial cells [29]. Tumor necrosis factor alpha (TNFa) is a multifunctional cytokine that is thought to have bimodal opposing effects on angiogenesis depending on its local concentration [33]. In the current study, hypercholesterolemia and oxLDL exposure led to increased expression of TNFa, which correlated *in vitro* with endothelial cell inflammatory activation, ROS production and impaired angiogenic activities. On the other hand, reduction of TNFa levels following treatment with miR-146b was associated with improvement of angiogenesis *in vitro* and ischemia-induced neovascularization in vivo, which is consistent with a previous study demonstrating that inhibition of TNFa can improve physiological angiogenesis in ischemic retinopathy [34]. Globally, our results suggest that reduced miR-146b expression in atherosclerotic conditions leads to activation of TRAF6-TNFa inflammatory pathway, which contributes to impair angiogenesis and ischemia-induced neovascularization.

The results of the present study suggest that PACs could also be involved in the modulation of neovascularization by miR-146b. PACs have been shown to reach ischemic tissues where they can improve neovascularization either directly by incorporating into new vessels, or more often indirectly through paracrine secretion of cytokines and angiogenic growth factors [16]. The number and the functional activities of PACs are reduced in hypercholesterolemic patients with or without apparent atherosclerotic diseases [20,35]. However, the specific mechanisms that are involved in the inhibition of PAC number and function by hypercholesterolemia are not completely understood. Here we found that treatment with miR-146b mimic following surgically-induced hindlimb ischemia could improve the number and the functional activities of PACs (proliferation, adhesion, integration into tubules) in hypercholesterolemic *ApoE*$^{-/-}$ mice. miRNAs are increasingly recognized as important regulators of stem and progenitor cells in the cardiovascular system [36]. The stimulating effect of miR-146b on PACs in the current study is consistent with previous reports demonstrating the importance of miR-146 family members as guardians of the quality and longevity of stem cells in mice [37] and for the angiogenic function of endothelial progenitor cells [38]. Similarly to what was found in mature endothelial cells, it is possible that TRAF6-TNFa inflammatory pathway is also involved in the modulation of bone marrow-derived PACs by miR-146b. For instance, TNFa has previously been shown to restrict hematopoietic stem cell activity in mice [39]. Moreover, overexpression of TRAF6 leads to hematopoietic stem cell defects [40]. Therefore it is plausible that miR-146b improves PAC functions by restraining the pro-inflammatory factors TRAF6 and TNFa, an effect that could be impaired in atherosclerotic conditions such as hypercholesterolemia. However, the precise mechanisms responsible for the modulation of PAC functions following intramuscular injection of miR-146b remain to be determined. miR-146b could recirculate and directly affect PACs in the bone marrow or, alternatively, PACs could be modulated indirectly due to systemic secretion of growth factors in mice injected with miR-146b.

In conclusion, our study demonstrates for the first time that reduced miR-146b expression contributes to impair angiogenesis and neovascularization in hypercholesterolemic conditions. The mechanism involves the activation of TRAF6-TNFa pro-inflammatory pathway, leading to reduced angiogenic activities of mature endothelial cells and PACs. Our results also suggest that forced expression of anti-inflammatory miR-146b using a miR mimic could represent a novel therapeutic strategy to improve neovascularization in ischemic vascular diseases.

Conflicts of interest

The authors declared they do not have anything to disclose regarding conflict of interest with respect to this manuscript.

Financial support

This study was supported by grants from the Canadian Institute of Health Research (CIHR MOP-123490) and the Heart and Stroke Foundation of Canada (HSFC G-17-0019106) to AR.

Author contributions

Conception and design: MD, AR; Analysis and interpretation: MD, SD, AR; Data collection: MD, SD, FR, SH, VS, SNH; Writing the article: MD, AR; Critical revision of the article: MD, SD, AR; Final approval of the article: MD, SD, FR, SH, VS, SNH, AR; Statistical analysis: MD, AR; Obtained funding: AR; Overall responsibility: MD, AR.

Appendix A. Supplementary data

Supplementary data to this article can be found online at https://doi.org/10.1016/j.atherosclerosis.2019.08.010.

References

[1] D. Steinberg, Atherogenesis in perspective: hypercholesterolemia and inflammation as partners in crime, Nat. Med. 8 (2002) 1211–1217.
[2] G.K. Hansson, Inflammation, atherosclerosis, and coronary artery disease, N. Engl. J. Med. 352 (2005) 1685–1695.
[3] P. Libby, P.M. Ridker, G.K. Hansson, et al., Inflammation in atherosclerosis: from pathophysiology to practice, J. Am. Coll. Cardiol. 54 (2009) 2129–2138.
[4] P.M. Ridker, B.M. Everett, T. Thuren, et al., Antiinflammatory therapy with canakinumab for atherosclerotic disease, N. Engl. J. Med. 377 (2017) 1119–1131.
[5] M.A. Gimbrone Jr., G. Garcia-Cardena, Endothelial cell dysfunction and the pathobiology of atherosclerosis, Circ. Res. 118 (2016) 620–636.
[6] R. Gareus, E. Kotsaki, S. Xanthoulea, et al., Endothelial cell-specific NF-kappaB inhibition protects mice from atherosclerosis, Cell Metabol. 8 (2008) 372–383.
[7] H.S. Cheng, N. Sivachandran, A. Lau, et al., MicroRNA-146 represses endothelial activation by inhibiting pro-inflammatory pathways, EMBO Mol. Med. 5 (2013) 1017–1034.
[8] K.D. Taganov, M.P. Boldin, K.J. Chang, et al., NF-kappaB-dependent induction of microRNA miR-146, an inhibitor targeted to signaling proteins of innate immune responses, Proc. Natl. Acad. Sci. U. S. A. 103 (2006) 12481–12486.
[9] L.J. Chen, L. Chuang, Y.H. Huang, et al., MicroRNA mediation of endothelial inflammatory response to smooth muscle cells and its inhibition by atheroprotective shear stress, Circ. Res. 116 (2015) 1157–1169.
[10] K. Li, D. Ching, F.S. Luk, et al., Apolipoprotein E enhances microRNA-146a in monocytes and macrophages to suppress nuclear factor-kappaB-driven inflammation and atherosclerosis, Circ. Res. 117 (2015) e1–e11.
[11] R. Echavarria, D. Mayaki, J.C. Neel, et al., Angiopoietin-1 inhibits toll-like receptor 4 signalling in cultured endothelial cells: role of miR-146b-5p, Cardiovasc. Res. 106 (2015) 465–477.
[12] D.W. Losordo, S. Dimmeler, Therapeutic angiogenesis and vasculogenesis for ischemic disease: part 1: angiogenic cytokines, Circulation 109 (2004) 2487–2491.
[13] P.A. D'Amore, R.W. Thompson, Mechanisms of angiogenesis, Annu. Rev. Physiol. 49 (1987) 453–464.
[14] T. Asahara, T. Murohara, A. Sullivan, et al., Isolation of putative progenitor endothelial cells for angiogenesis, Science 275 (1997) 964–967.
[15] T. Asahara, H. Masuda, T. Takahashi, et al., Bone marrow origin of endothelial progenitor cells responsible for postnatal vasculogenesis in physiological and pathological neovascularization, Circ. Res. 85 (1999) 221–228.
[16] C. Urbich, S. Dimmeler, Endothelial progenitor cells: characterization and role in vascular biology, Circ. Res. 95 (2004) 343–353.
[17] E. Van Belle, A. Rivard, D. Chen, et al., Hypercholesterolemia attenuates angiogenesis but does not preclude augmentation by angiogenic cytokines, Circulation 96 (1997) 2667–2674.
[18] T. Couffinhal, M. Silver, M. Kearney, et al., Impaired collateral vessel development associated with reduced expression of vascular endothelial growth factor in ApoE-/- mice, Circulation 99 (1999) 3188–3198.
[19] D. Tirziu, K.L. Moodie, Z.W. Zhuang, et al., Delayed arteriogenesis in hypercholesterolemic mice, Circulation 112 (2005) 2501–2509.
[20] J.Z. Chen, F.R. Zhang, Q.M. Tao, et al., Number and activity of endothelial progenitor cells from peripheral blood in patients with hypercholesterolaemia, Clin. Sci. (Lond.) 107 (2004) 273–280.
[21] M. Desjarlais, S. Dussault, W. Dhahri, et al., MicroRNA-150 modulates ischemia-induced neovascularization in atherosclerotic conditions, Arterioscler. Thromb. Vasc. Biol. 37 (2017) 900–908.
[22] F. Maingrette, S. Dussault, W. Dhahri, et al., Psychological stress impairs ischemia-induced neovascularization: protective effect of fluoxetine, Atherosclerosis 241 (2015) 569–578.
[23] B.H. Annex, Therapeutic angiogenesis for critical limb ischaemia, Nat. Rev. Cardiol. 10 (2013) 387–396.
[24] M.R. Paterson, A.J. Kriegel, MiR-146a/b: a family with shared seeds and different

roots, Physiol. Genom. 49 (2017) 243–252.
[25] K. Zhu, Q. Pan, X. Zhang, et al., MiR-146a enhances angiogenic activity of endothelial cells in hepatocellular carcinoma by promoting PDGFRA expression, Carcinogenesis 34 (2013) 2071–2079.
[26] H.Y. Zhu, W.D. Bai, J.Q. Liu, et al., Up-regulation of FGFBP1 signaling contributes to miR-146a-induced angiogenesis in human umbilical vein endothelial cells, Sci. Rep. 6 (2016) 25272.
[27] Y. Li, H. Zhu, X. Wei, et al., LPS induces HUVEC angiogenesis *in vitro* through miR-146a-mediated TGF-beta1 inhibition, Am J Transl Res 9 (2017) 591–600.
[28] N. Stickel, G. Prinz, D. Pfeifer, et al., MiR-146a regulates the TRAF6/TNF-axis in donor T cells during GVHD, Blood 124 (2014) 2586–2595.
[29] S. Bruneau, D. Datta, J.A. Flaxenburg, et al., TRAF6 inhibits proangiogenic signals in endothelial cells and regulates the expression of vascular endothelial growth factor, Biochem. Biophys. Res. Commun. 419 (2012) 66–71.
[30] J.S. Silvestre, Z. Mallat, A. Tedgui, et al., Post-ischaemic neovascularization and inflammation, Cardiovasc. Res. 78 (2008) 242–249.
[31] C.M. Coughlin, K.E. Salhany, M. Wysocka, et al., Interleukin-12 and interleukin-18 synergistically induce murine tumor regression which involves inhibition of angiogenesis, J. Clin. Investig. 101 (1998) 1441–1452.
[32] H.G. Kopp, A.T. Hooper, M.J. Broekman, et al., Thrombospondins deployed by thrombopoietic cells determine angiogenic switch and extent of revascularization, J. Clin. Investig. 116 (2006) 3277–3291.
[33] L.F. Fajardo, H.H. Kwan, J. Kowalski, et al., Dual role of tumor necrosis factor-alpha in angiogenesis, Am. J. Pathol. 140 (1992) 539–544.
[34] T.A. Gardiner, D.S. Gibson, T.E. de Gooyer, et al., Inhibition of tumor necrosis factor-alpha improves physiological angiogenesis and reduces pathological neovascularization in ischemic retinopathy, Am. J. Pathol. 166 (2005) 637–644.
[35] M. Vasa, S. Fichtlscherer, A. Aicher, et al., Number and migratory activity of circulating endothelial progenitor cells inversely correlate with risk factors for coronary artery disease, Circ. Res. 89 (2001) E1–7.
[36] E.M. Heinrich, S. Dimmeler, MicroRNAs and stem cells: control of pluripotency, reprogramming, and lineage commitment, Circ. Res. 110 (2012) 1014–1022.
[37] J.L. Zhao, D.S. Rao, R.M. O'Connell, et al., MicroRNA-146a acts as a guardian of the quality and longevity of hematopoietic stem cells in mice, Elife 2 (2013) e00537.
[38] Z.F. Su, Z.W. Sun, Y. Zhang, et al., Regulatory effects of miR-146a/b on the function of endothelial progenitor cells in acute ischemic stroke in mice, Kaohsiung J. Med. Sci. 33 (2017) 369–378.
[39] C.J. Pronk, O.P. Veiby, D. Bryder, et al., Tumor necrosis factor restricts hematopoietic stem cell activity in mice: involvement of two distinct receptors, J. Exp. Med. 208 (2011) 1563–1570.
[40] J. Fang, L.C. Bolanos, K. Choi, et al., Ubiquitination of hnRNPA1 by TRAF6 links chronic innate immune signaling with myelodysplasia, Nat. Immunol. 18 (2017) 236–245.